BROOKHAVEN
NATIONAL LABORATORY

BNL-79414-2007-CP

Bernas ion source discharge simulation

I. Rudskoy[1], T.V. Kulevoy[1], S.V. Petrenko[1], R.P. Kuibeda[1], D.N. Seleznev[1], V.I. Pershin[1], A. Hershcovitch[2], B.M. Johnson[2], V.I. Gushenets[3], E.M. Oks[3], H.J. Poole[4]

[1]*Institute for Theoretical and Experimental Physics, Moscow, 117218, Russia*
[2]*Brookhaven National Laboratory, Upton, NY 11973, USA*
[3]*High Current Electronics Institute Russian Academy of Sciences, Tomsk, 634055 Russia*
[4]*PVI, Oxnard, CA 93031-5023, USA*

Presented at the 12th International Conference on Ion Sources (ICIS 2007)
Jeju, Korea
August 26 – 31, 2007

Collider-Accelerator Department
Brookhaven National Laboratory
P.O. Box 5000
Upton, NY 11973-5000
www.bnl.gov

DISCLAIMER

Bernas Ion Source Discharge Simulation*a)

I. Rudskoy[1], T.V. Kulevoy[1], S.V. Petrenko[1], R.P. Kuibeda[1], D.N. Seleznev[1], V.I. Pershin[1], A. Hershcovitch[2], B.M. Johnson[2], V.I. Gushenets[3], E.M. Oks[3], H.P. Poole[4].

[1] Institute for Theoretical and Experimental Physics, Moscow 117218, Russia

[2] Brookhaven National Laboratory, Upton, New York 11973, USA

[3] High Current Electronics Institute Russian Academy of Sciences, Tomsk, 634055 Russia

[4] PVI, Oxnard, California 93031-5023, USA

Fax: +7-(495)-123-3028 E-mail address: kulevoy@itep.ru

Abstract. The joint research and development program is continued to develop steady-state ion source of decaborane beam for ion implantation industry. Bernas ion source is the wide used ion source for ion implantation industry. The new simulation code was developed for the Bernas ion source discharge simulation. We present first results of the simulation for several materials interested in semiconductors. As well the comparison of results obtained with experimental data obtained at the ITEP ion source test-bench is presented.

Introduction

The joint research and development program is continued to develop steady-state ion source for ion implantation industry. Bernas ion source is the wide used ion source for ion implantation industry. Therefore, in framework of investigation of low energy beam generation for ion implantation, we use ITEP version of Bernas ion source [1] - [3]. As the technology and applications continue to grow, there is a need for development of plasma and ion sources with clearly specified characteristic. Manufacturing sources of this kind at present could not be accomplished without comprehensive numerical studies at the project stage. It is even more important when the ion source for low energy implantation is developed. Universal plasma models based on Vlasov-Boltzmann equation can be used to describe a wide variety of these

---

* This work was supported by the DOE IPP Trust 2 program. (CRDF GAP Grant # RPO 10225 – BNL)

a) Contributed paper, published as part of the Proceedings of the 12th International Conference on Ion Sources, Jeju, Korea, August 2007

sources. Recently the most commonly encountered numerical approach to solve this equation is the Monte-Carlo Particle-In-Cell (MCPIC) method also known as Particle-In-Cell method with Monte-Carlo collisions. In this paper we present the 2D3V numerical code **PICSIS-2D** realizing MCPIC method and the results of simulations as applied to Bernas ion sources. The numerical results are compared with experimental data.

Simulation model

Plasma filling an ion source is supposed to consist of electrons and different kinds of ions of all charge states, which are represented by distribution functions $f_k(\vec{x},\vec{v},t)$, where $\vec{x}$ is the particle position and $\vec{v}$ is the particle velocity. As usual the distribution functions f_k give the probability of finding particles of sort k in a given volume of phase space. The electrons and ions in the plasma under consideration are assumed to interact via electric $\vec{E}$ fields, static magnetic $\vec{B}$ fields and binary collisions. The neutral gas is treated as a uniform background of atoms or molecules with a constant temperature.

An appropriate equation set can be written as follows:

$$\frac{df_k}{dt} = \frac{\partial f_k}{\partial t} + \vec{v}\frac{\partial f_k}{\partial \vec{x}} + \frac{\vec{F}_k}{m_k}\frac{\partial f_k}{\partial \vec{v}} = I_c$$

Here m_k is the particle mass. The right-hand member I_c in this equation is the collision integral which defines changes of distribution functions f_k under collisions. The following electron collisions are included into consideration: elastic electron-electron, electron-ion and electron-neutral collisions; and inelastic ionizing and exciting collisions with neutrals and ions. Ion collisions included are elastic ion-neutral collisions and charge exchange collisions.

The force $\vec{F}_k$ on the particles with the charge q_k is the Lorentz force given by:

$$\vec{F}_k = q_k(\vec{E} + \vec{v} \times \vec{B})$$

The electric field $\vec{E}$ appeared in the equation is defined by plasma self-field and external electrodes. It is obtained from solution of the Poisson equation:

$$\vec{\nabla} \cdot \vec{E} = 4\pi\rho$$

The static external magnetic field $\vec{B}$ should be calculated as a preliminary in analytical or numerical ways. It can be set also as an experimental data table. The time varying magnetic field induced by currents of charged particles is neglected here since for the problem involved it is much smaller than other forces acting on the particles.

The Monte-Carlo Particle-In-Cell numerical approach chosen for solving the equations makes use of finite elements or quasi-particles to represent the distribution functions f_k. Each finite particle stands for the group of physical particles and has a mass and charge accordingly to the type of ions or electrons. Trajectories of these particles in phase space represent the evolution of the respective distribution functions and can be found by time integrating of the motion equations:

$$m_k \frac{d\vec{v}}{dt} = q_k(\vec{E} + \vec{v} \times \vec{B}), \qquad \vec{x} = \frac{d\vec{v}}{dt}$$

These two equations are solved using explicit time-centered leapfrog [4], [5]. A spatial grid (or mesh) overlaying all of the particles is used in order to calculate charge densities ρ at the grid points from the particle positions (so-called charge weighting to grid). These densities are then used to solve the Poisson equation on the grid. Then the particles forces are interpolated from the grid (so-called field weighting to particles). The code provides various interpolated functions for charge and force: zero-, first- and second-order splines depending on the problem under consideration. The solution of Poisson equation is found by the double fast Fourier transformation [6] in a 2D frame of reference (plane or cylindrical). The Dirichlet boundary conditions are used at conductive surfaces with known potentials and the Neumann conditions – at the axis (in case of cylindrical geometry). These tree procedures: charge weighting, field calculation and force weighting are performed at an every integration step to provide a self-consistent solution of these equations.

The collisions events are modeled using a Monte-Carlo technique, where random numbers are used to choose a time between collisions, to pick a particular event and to define post collision velocities. Depending on collision frequencies we use an approach proposed [4] (if a cumulative probability at an integration step >0.01), or a simplified scheme [7] - in the opposite case. To shorten consumption time an *ad hoc* table of collision frequencies is generated in the beginning of simulation.

Elastic collisions with neutrals are regarded in hard sphere approximation. For inelastic collisions the respective analytical or experimental differential cross-sections are applied. Binary collisions of charged particles are regarded in the way described by [8], [9]. To define an interaction range for colliding particles we use the same mesh as on solution of the Poisson equation. Small-angle scattering probabilities are supposed to follow the well-known Spitzer equation [10].

Numerical results

At first, the model described above was tested on the problems having analytical solutions: the development of two-beam instability, the ion charge state relaxation, the drift in crossed electric and magnetic fields, the momentum isotopization and establishing of thermal equilibrium in plasmas. After that, it has been applied to the simulation of DC glow discharge. We have simulated the development of DC glow discharge in a tube of 20cm long and 1 cm in diameter filled with hydrogen under the pressure of 0.2 torr. It was assumed that the voltage of 1200V was applied through the resistor of 10^7 Ohm to the platinum electrodes. Elastic scattering, ionization and excitation of vibration, rotation and main electronic levels were taken into account as well as secondary electron emission from the cathode under ion impacts. All particles reaching the walls or electrodes are considered as killed.

To initiate the discharge we have supposed that the cathode can emit electrons with the temperature of filament (~0.1eV). About 10^6 finite particles were under consideration.

The results obtained are depicted in Fig. 1 – Fig. 3. In 5 μs after the beginning the discharge became stabilize and steady state discharge current remain approximately the same during all computational time (up to 50 μs). Since the total light emission usually follows the electron density one can see the most intensive negative glow and a stratified positive column. The values of cathode drop U_c (~ 280 V) and the thickness of cathode layer d_c (~ 5.1cm) good agree with tabulated experimental data – 276 V and 5 cm respectively. Moreover in the Fig. 3 one can see that the strata are not stable and run towards the cathode in accordance with experimental observations. The more fine structure of the discharge (Aston and cathode dark spaces) can be also distinguished by analyzing of electron energy distribution.

Finally, the code has been applied for simulation of Bernas ion sources. Schematic sketch of an ion source is shown in Fig. 4. It was found that there are different modes of ion source operating. One of them does not lead to arising of self-sustaining discharge (see Fig. 5 and Fig. 6) due to significant suppression of electron emission by the negative space charge. Another one initiates a discharge shown in Fig. 7 – Fig. 10. In this case we have used for simulation the real parameters of the ion source operating in ITEP, Moscow [1]. Both the steady-state value of current discharge (I_d=260mA) and the current of the extracted ions (I_1=10mA for Sb^{+1}) are in a good agreement with experimental data [3].

Conclusion

The results obtained clearly confirm that the numerical code depicted in this paper represents an adequate model of physical processes in the wide range of ion source plasmas. It can be successfully used for ion source development for low energy implantation. As well it can

be used in the course for development of various kinds discharge ion sources. For example, we hope that after some modifications and improvements undertaking at present time it will work for ECR ion sources modeling.

Acknowledgements

This work was supported by the DOE IPP Trust 2 program. (CRDF GAP Grant # RPO 10225 – BNL).

References

[1] A. Hershcovitch, V. A. Batalin, A. S. Bugaev, V. I. Gushenets, B. M. Johnson, A. A. Kolomiets, G. N. Kropachev, R. P. Kuibeda, T. V. Kulevoy, I. V. Litovko, E. S. Masunov, E. M. Oks, V. I. Pershin, S. V. Petrenko, S. M. Polozov, H. J. Poole, I. Rudskoy, D. N. Seleznev, P. A. Storozhenko, A. Ya. Svarovski, G. Yu. Yushkov, Ion sources for the varying needs of ion implantation, Rev. Sci. Instrum. 77, 03B510 (2006)

[2] T. V. Kulevoy, S. V. Petrenko, R. P. Kuibeda, V. A. Batalin, V. I. Pershin, A. V. Koslov, Yu. B. Stasevich, A. Hershcovitch, H. J. Poole, E. M. Oks, V. I. Gushenets, H. J. Poole, P. A. Storozhenko, E. L. Gurkova, O. V. Alexeenko, Decaborane beam from ITEP Berna ion source – RSI, Rev. Sci. Instrum. 77(3) 03C102 (2006)

[3] T. V. Kulevoy, R. P. Kuibeda, S. V. Petrenko, V. A. Batalin, V. I. Pershin, G. N. Kropachev, A. Hershcovitch, B. M. Johnson, V. I. Gushenets, E. M. Oks, H. J. Poole, ITEP Berna IS with additional e-beam – RSI, Rev. Sci. Instrum. 77(3) 03C110 (2006)

[4] R.W. Hockney and J.W. Eastwood, Computer Simulation Using Particles, New York: McGraw-Hill, 1981

[5] J. P. Boris, K.V. Roberts, J. Comput. Phys, v. 4, pp. 552-571, 1969

[6] M.H.Hughes, Comput. Phys. Commun., v.2, pp.157-167, 1971

[7] C.K.Birdsall, IEEE Trans. Plasma Sci., v. 19, pp. 65-85, 1991

[8] T. Takizuka and H. Abe, J. Comput. Phys, v. 25, p. 205-219, 1977

[9] J.M. Dawson, S. Ma, R.D. Sydora, Comput. Phys. Commun., v. 77, pp. 190-195, 1993

[10] L.Spitzer, Physics of Fully Ionised Gases, New York, Wiley-Interscience, 1962.

Figures.

Fig. 1 Electron density distribution along the discharge. Position of the anode x=0; cathode – x=20 cm

Fig. 2 The distribution of potential along the discharge. Position of the anode x=0; cathode – x=20 cm.

Fig. 3 Time evolution of electron density

Fig. 4 Pictorial description of the Berna's ion source. Blue – cathode and anticathode, Black – anode, U – discharge voltage, B – magnetic field, I_{em} – electrons' flow cathode to plasma, I_e – electrons' flow from plasma to anode, I_i – ions flow from plasma to electrodes.

Fig. 5 Electric field distributions in the ion source vs time: a) longitudinal b) radial.

Sb, L=5cm; R=1cm; $n_0=10^{13}$ cm^{-3}; B=2 kGs; U=280 V; T_{em}=2700K.

Fig. 6. 2D distribution of the electric field vs time. a) initial distribution; b) 0.1μs; c) 0.5 μs; d) 2 μs

Fig. 7 Electric field distributions in the ion source vs time: a) longitudinal b) radial. Sb, L=5cm; R=0.5 cm; $n_0=10^{13}$ cm^{-3}; B=600Gs; U=280 V; T_{em}=2700K.

Fig. 8. 2D distribution of the electric field vs time. a) initial distribution; b) 1μs; c) 3 μs; d) 5 μs

Fig. 9. Steady-state electric field distribution t=10 μs

Fig. 10 Steady-state 2D distribution of the electric field. a) 5 μs; b) 10 μs; c) 15 μs; d) 20 μs

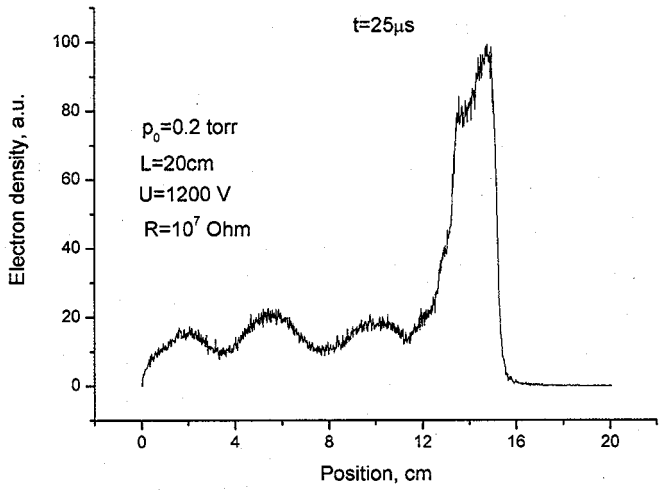

Fig. 1. Electron density distribution along the discharge.

Position of the anode x=0; cathode – x=20 cm

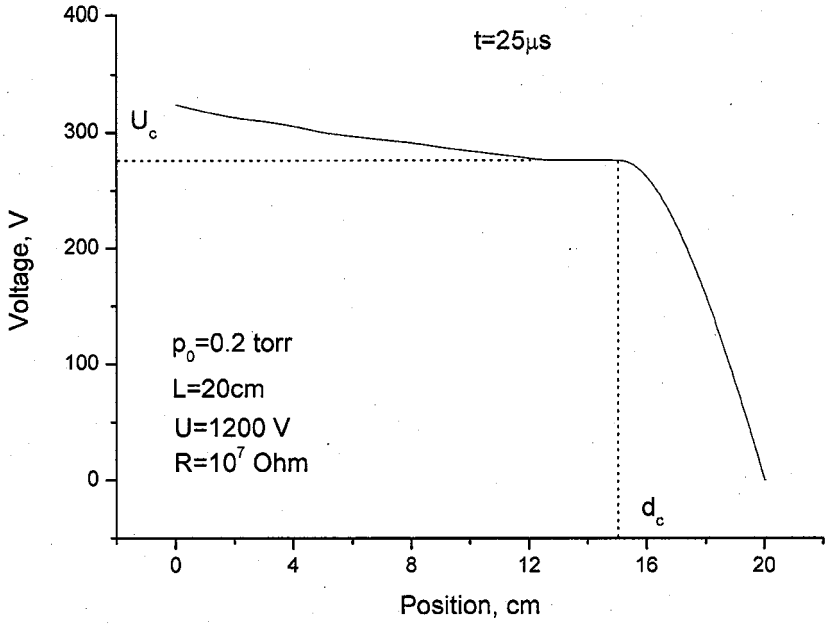

Fig. 2. The distribution of potential along the discharge.

Position of the anode x=0; cathode – x=20 cm

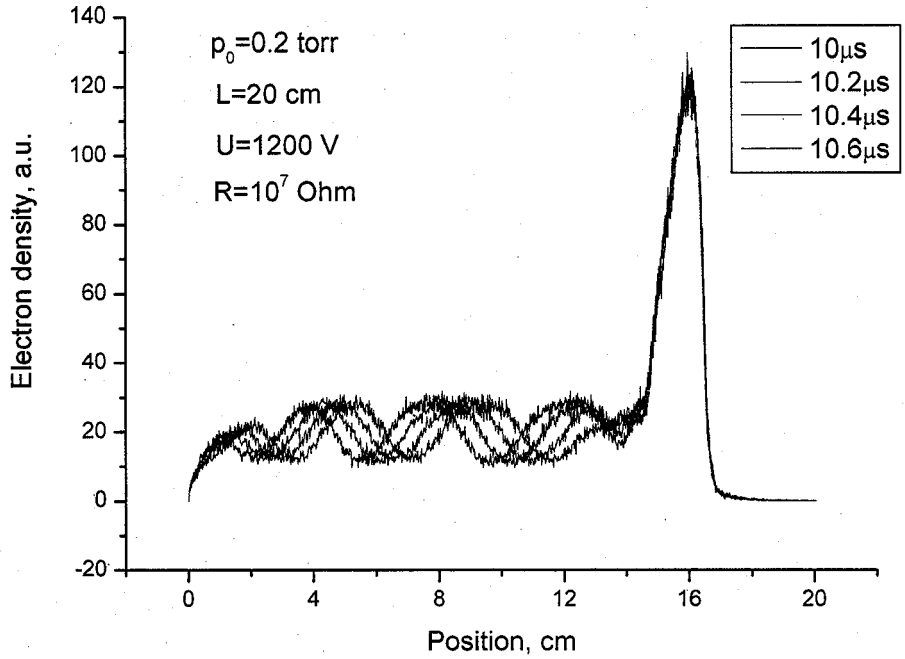

Fig. 3 Time evolution of electron density

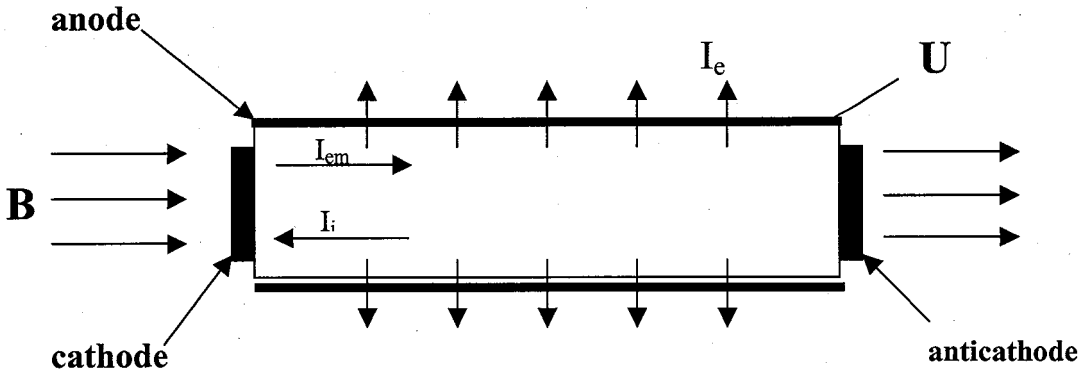

Fig.4 Sketch of a Berna's ion source.
B – magnetic field, U – discharge voltage, I_{em} – electrons flow from cathode to plasma, I_i – ion flow from plasma, I_e – electron flow from plasma to anode.

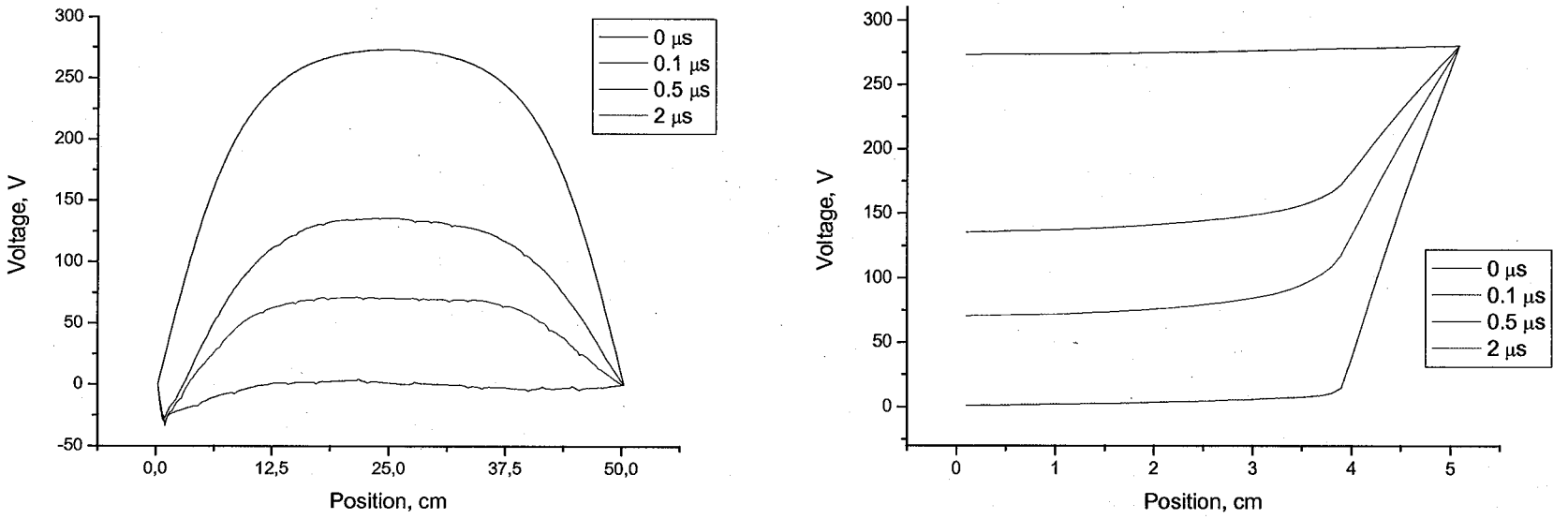

Fig. 5. Electric field distributions in the ion source vs time:

a) longitudinal b) radial.Sb, L=5cm; R=1cm; $n_0=10^{13}$ cm^{-3}; B=2 kGs; U=280 V; T_{em}=2700K.

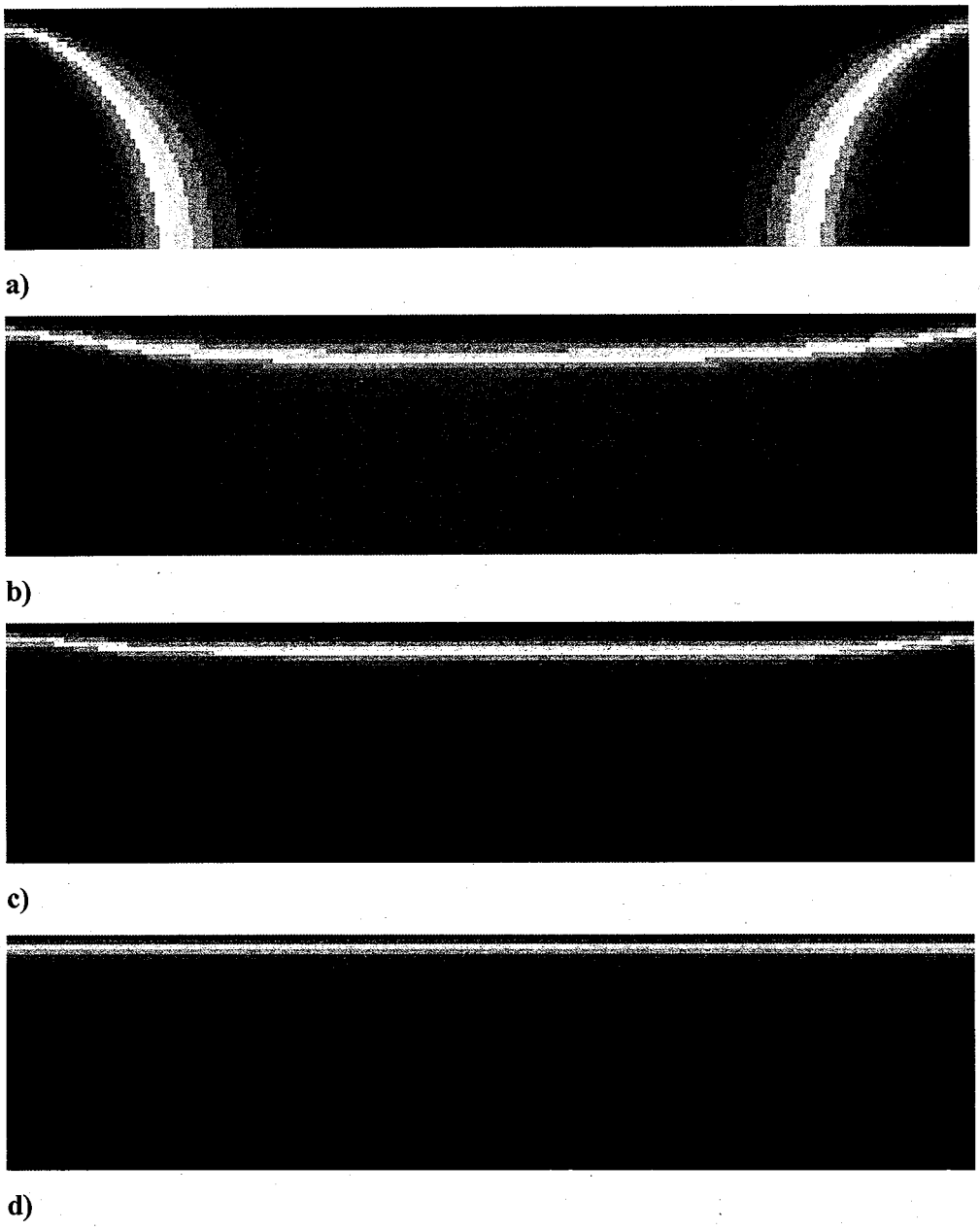

Fig. 6. 2D distribution of the electric field vs time.
a) initial distribution; b) 0.1μs; c) 0.5 μs; d) 2 μs

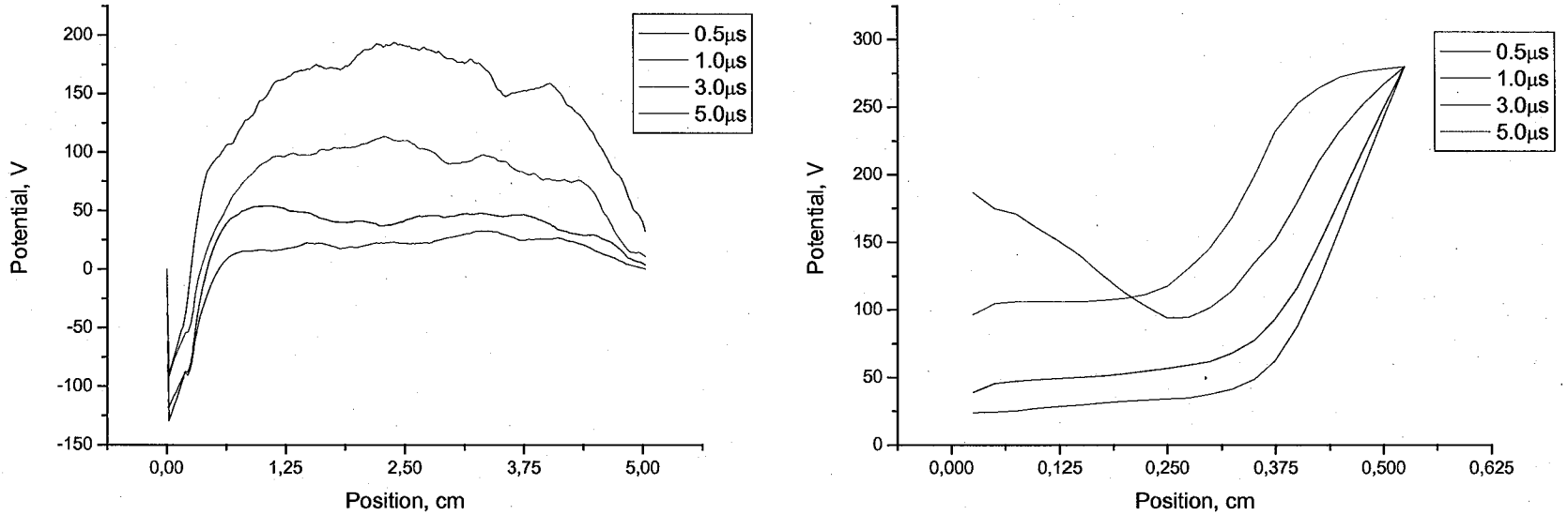

Fig. 7. Electric field distributions in the ion source vs time: a) longitudinal b) radial.

Sb, L=5cm; R=0.5 cm; $n_0=10^{13}$ cm^{-3}; B=600Gs; U=280 V; T_{em}=2700K.

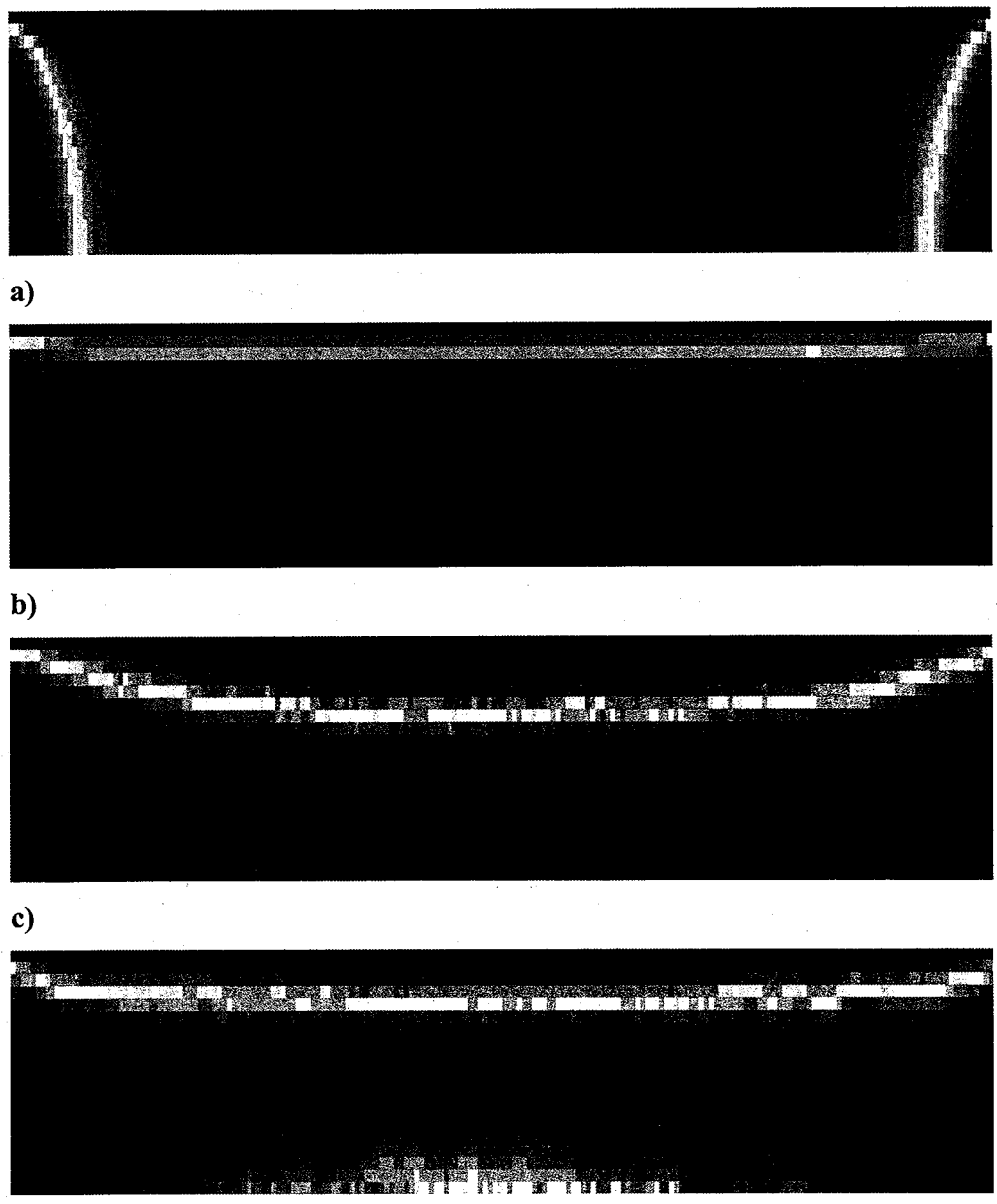

Fig. 8 2D distribution of the electric field vs time.

a) initial distribution; b) 1μs; c) 3 μs; d) 5 μs

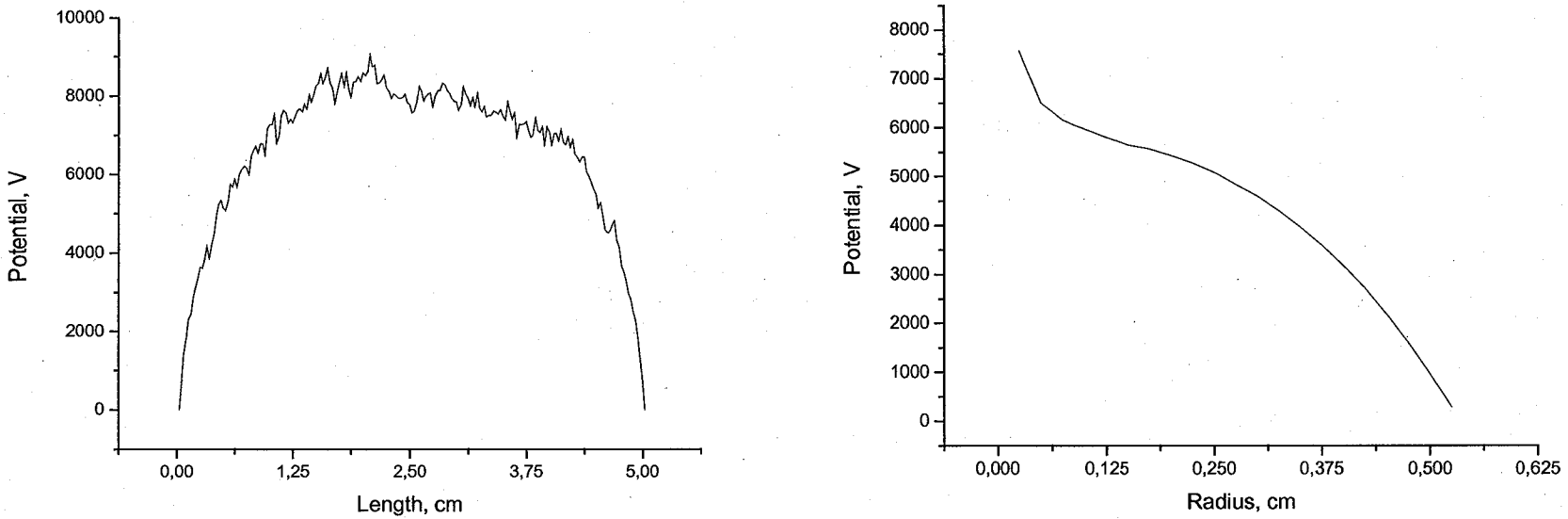

Fig. 9. Steady-state electric field distribution t=10 μs

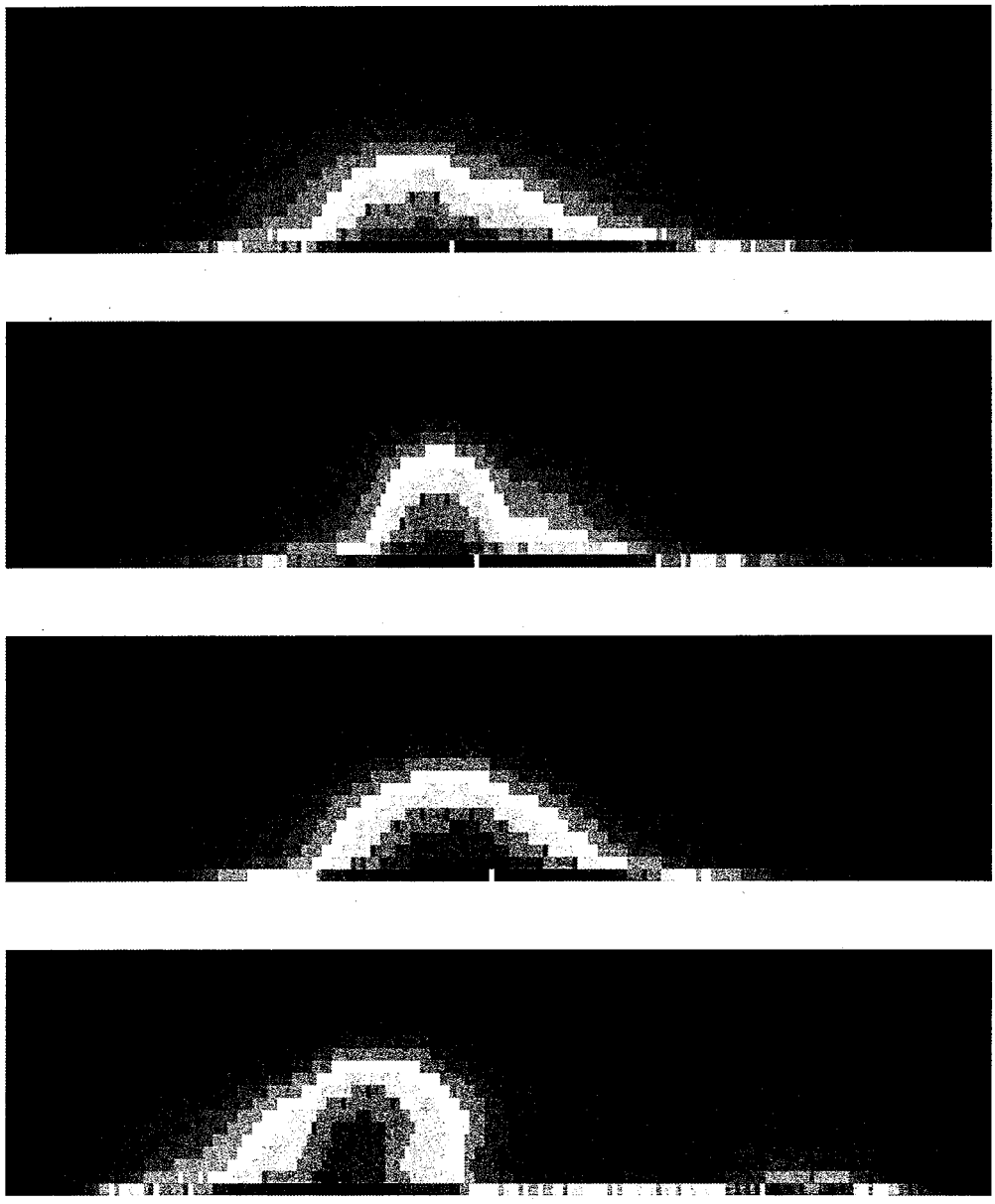

Fig. 10. Steady-state 2D distribution of the electric field.
a) 5 μs; b) 10 μs; c) 15 μs; d) 20 μs